

# 8-Hydroxy-1,6-naphthyridine-7-carboxamides as Inhibitors of Human Cytomegalovirus pUL89 Endonuclease

Eunkyung Jung,<sup>[a]</sup> Ryuichi Majima,<sup>[a]</sup> Tiffany C. Edwards,<sup>[a]</sup> Ruben Soto-Acosta,<sup>[a]</sup> Robert J. Geraghty,<sup>[a]</sup> and Zhengqiang Wang\*<sup>[a]</sup>

Human cytomegalovirus (HCMV) replication requires a metal-dependent endonuclease at the C-terminus of pUL89 (pUL89-C) for viral genome packaging and cleavage. We have previously shown that pUL89-C can be pharmacologically inhibited with designed metal-chelating compounds. We report herein the synthesis of a few 8-hydroxy-1,6-naphthyridine subtypes, including 5-chloro (subtype 15), 5-aryl (subtype 16), and 5-amino (subtype 17) variants. Analogs were studied for the inhibition of pUL89-C in a biochemical endonuclease assay, a biophysical thermal shift assay (TSA), *in silico* molecular docking,

and for the antiviral potential against HCMV in cell-based assays. These studies identified eight analogs of 8-hydroxy-1,6-naphthyridine-7-carboxamide subtypes for further characterization, most of which inhibited pUL89-C with single-digit  $\mu\text{M}$   $\text{IC}_{50}$  values, and conferred antiviral activity in  $\mu\text{M}$  range. TSA and molecular modeling of selected analogs corroborate their binding to pUL89-C. Collectively, our biochemical, antiviral, biophysical and *in silico* data suggest that 8-hydroxy-1,6-naphthyridine-7-carboxamide subtypes can be used for designing inhibitors of HCMV pUL89-C.

## Introduction

Human cytomegalovirus (HCMV) is a  $\beta$ -herpesvirus that infects the majority of the world population and causes severe diseases in newborns,<sup>[1–3]</sup> organ transplant recipients,<sup>[4]</sup> and human immunodeficiency virus type 1 (HIV-1) co-infected individuals.<sup>[5–6]</sup> Direct-acting antivirals (DAAs) have been developed for treating HCMV infections (Figure 1), including polymerase inhibitors ganciclovir (GCV, 1),<sup>[7]</sup> the primary treatment option,<sup>[8]</sup> cidofovir (CDV, 2),<sup>[9]</sup> and foscarnet (FOS, 3);<sup>[10]</sup> terminase inhibitor letermovir (LTV, 4),<sup>[11]</sup> and the recently approved maribavir (MBV, 5),<sup>[12]</sup> a viral kinase pUL97 inhibitor.<sup>[13]</sup> However, polymerase inhibitors 1–3 are associated with dose-related adverse effects, and LTV is approved only for HCMV prophylaxis in stem cell recipients. In addition, clinical resistance mutations have been observed with all these drugs, including MBV.<sup>[14–17]</sup> Therefore, there remains a pressing need to develop mechanistically novel HCMV drugs.

We are particularly interested in the viral terminase complex (TC),<sup>[18]</sup> a drug target<sup>[19]</sup> clinically validated by the approval of LTV. The TC minimally consists of a guide protein (pUL56) and an ATPase/endonuclease (pUL89). TC cleaves concatemeric HCMV DNA into unit-length genomes for DNA packaging, and

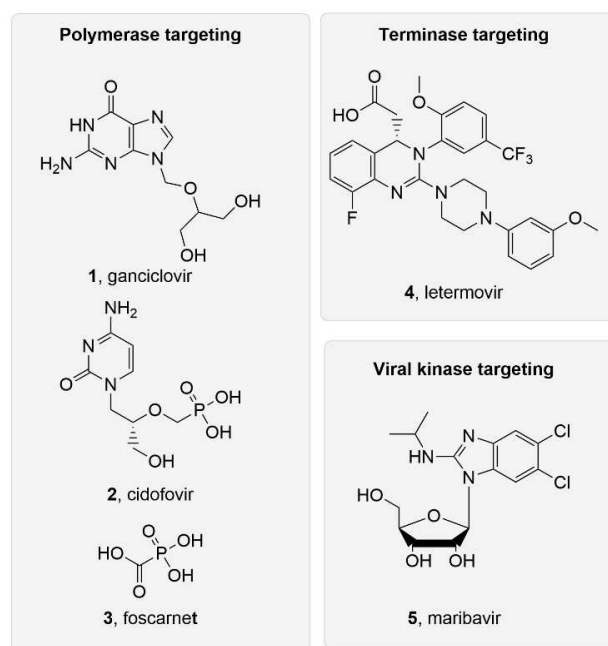


Figure 1. Current FDA-approved HCMV drugs include polymerase inhibitors 1–3, terminase complex inhibitor 4 and viral kinase inhibitor 5.

thus is required for productive viral replication. It is noteworthy that while key LTV resistance mutations have largely been mapped to UL56,<sup>[11]</sup> pUL89 remains underexplored for HCMV drug discovery. If developed, pUL89-targeting antivirals will constitute a new drug class, and could be used in combination with current drugs. Interestingly, the C-terminus of the component protein pUL89 (pUL89-C) houses a divalent metal-dependent endonuclease activity (Figure 2, A).<sup>[20]</sup> The RNase H-like active site structural fold and the metal-dependent catalytic mechanism of pUL89-C are shared by a few other viral metallo

[a] Dr. E. Jung, Dr. R. Majima, Dr. T. C. Edwards, Dr. R. Soto-Acosta, Prof. Dr. R. J. Geraghty, Prof. Dr. Z. Wang  
Center for Drug Design,  
College of Pharmacy  
University of Minnesota, Minneapolis, MN 55455 (USA)  
E-mail: wangx472@umn.edu

Supporting information for this article is available on the WWW under <https://doi.org/10.1002/cmdc.202200334>

© 2022 The Authors. ChemMedChem published by Wiley-VCH GmbH. This is an open access article under the terms of the Creative Commons Attribution Non-Commercial License, which permits use, distribution and reproduction in any medium, provided the original work is properly cited and is not used for commercial purposes.

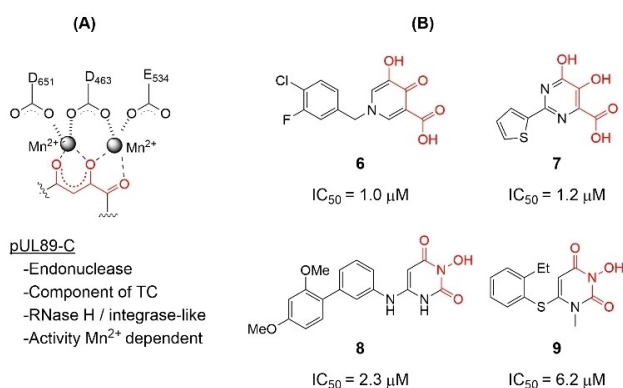


**Figure 2.** pUL89-C as an antiviral target. (A) The metal-dependent endonuclease activity of pUL89-C is required by the terminase complex (TC), with the active site featuring a DDE motif chelating two  $Mn^{2+}$  ions; (B) Previously reported metal-binding inhibitor types of HCMV pUL89-C. All inhibitors entail a chelating triad comprising three O atoms (highlighted in red) and inhibit pUL89-C in an ELISA biochemical assay with  $IC_{50}$  values in the low  $\mu M$  range.

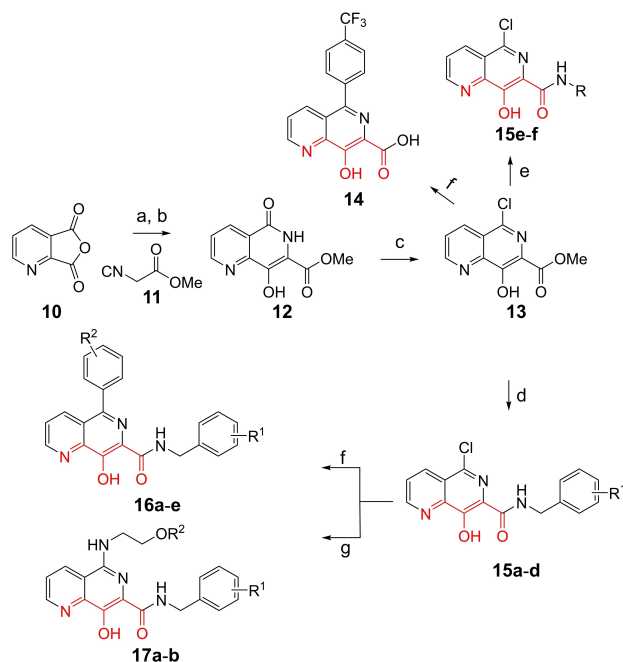
enzymatic functions<sup>[21–22]</sup> we have targeted, including HIV-1 integrase strand transfer (INST),<sup>[23–25]</sup> HIV-1 reverse transcriptase-associated ribonuclease H (RNase H),<sup>[26–34]</sup> hepatitis B virus (HBV) RNase H,<sup>[35]</sup> and hepatitis C virus (HCV) NS5B.<sup>[36–37]</sup> Along the same line, our prior research has identified and characterized a few metal-binding pUL89-C inhibitor types (Figure 2, B): hydroxypyridine carboxylic acid (HPCA, **6**),<sup>[38–39]</sup> dihydropyrimidine (DHP) carboxylic acid (**7**),<sup>[40]</sup> 6-arylamino-3-hydroxypyrimidine-2,4-dione (HPD-NH, **8**),<sup>[41]</sup> and the 6-arylthio-3-hydroxypyrimidine-2,4-dione (HPD-S, **9**),<sup>[42]</sup> Notably, inhibitor types **6–9** all feature a chelating triad comprising three oxygen atoms for binding two  $Mn^{2+}$  ions (Figure 2, B, red).

To gain better understanding on pUL89-C inhibition, we surveyed metal-chelating chemotypes bearing a chelating triad that may include a non-oxygen heteroatom, such as nitrogen. Toward this end, we turned our attention to 8-hydroxy-1,6-naphthyridine-7-carboxamide which contains one nitrogen atom in its chelating triad (Scheme 1) and has been extensively explored as an important inhibitor type of HIV-1 INST.<sup>[43–49]</sup> Specifically, we synthesized and tested 5-chloro (subtype **15**), 5-aryl (subtype **16**), and 5-amino (subtype **17**) variants of the 8-hydroxy-1,6-naphthyridine-7-carboxamide chemotype, along with an acid analog **14** (Scheme 1).

## Results and Discussion

### Chemical synthesis

All analogs tested in the current studies were synthesized as depicted in Scheme 1 from quinolinic anhydride (**10**) through two key intermediates, the 5-oxo-naphthyridine **12** and the 5-chloro-naphthyridine **13** (Scheme 1). In the synthetic event, the condensation between quinolinic anhydride (**10**) and methyl 2-isocynoacetate (**11**) afforded the cyclized intermediate ester **12**, which was converted into chloride **13** upon treatment with  $POCl_3$ . Direct aminolysis of ester **13** under two distinct sets of



**Scheme 1.** Synthesis of 8-hydroxy-1,6-naphthyridine subtypes **14–17**. Reagents and conditions: a) DBU, THF, 40 °C; b) HCl (Conc.), 55 °C, 18 h, 56%, over-2-steps; c)  $POCl_3$ , MW, 130 °C, 30 min, 85%; d)  $R^1NH_2$ , AcOH, toluene, 110 °C, 18 h, 43–65%; e)  $R^1NH_2$ , NaOMe, DMSO, 110 °C, 43–52%; f)  $ArB(OH)_2$ ,  $Pd(PPh_3)_4$ ,  $K_2CO_3$ ,  $CH_3CN$ , MW, 150 °C, 30 min, 37–69%; g)  $NH_2(CH_2)_2OR_2$ , 150 °C, 18 h, 39–49%.

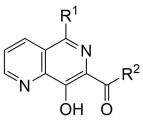
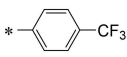
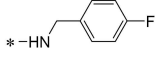
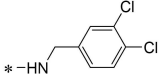
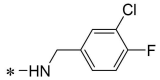
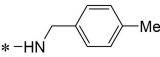
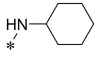
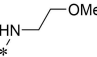
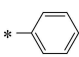
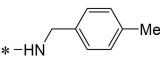
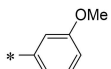
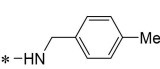
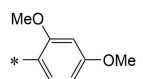
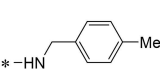
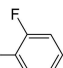
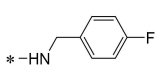
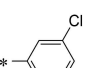
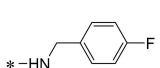
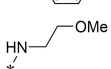
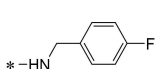
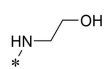
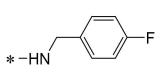
conditions (d and e) produced **15a–d**, and **15e–f**, respectively. The former subtype (**15a–d**) was further diversified to deliver 5-phenyl substituted analogs **16a–e** via Suzuki coupling (step f). Amination of **15a–d** under heating yielded 5-amino analogs **17a–b** (step g). Interestingly, when the same Suzuki coupling condition was applied to intermediate **13**, a hydrolyzed product, acid **14** was obtained to serve as an important variant for structure-activity relationship (SAR).

### Biochemical and antiviral testing

Compounds were evaluated mainly in a biochemical endonuclease assay, and cell-based antiviral and cytotoxicity assays. All analogs were first screened in these assays at 10  $\mu M$ . Those with large inhibition % from both the biochemical and antiviral assays, and viability % from the cell-based assays, were further tested in a dose-response fashion where  $IC_{50}$ ,  $EC_{50}$  and  $CC_{50}$  values were calculated. Selected analogs were also studied in a biophysical thermal shift assay (TSA) and molecular docking to assess target binding.

The screening against pUL89-C was conducted in an endonuclease biochemical assay measuring the cleavage of the DNA substrate. Previously reported pUL89-C inhibitor **6** was included on each plate as the control. As shown in Table 1, non-amide subtypes, including 5-oxonaphthyridine ester (**12**, inhibition % = 14), 5-chloronaphthyridine ester (**13**, inhibition % = 16), and 5-phenylnaphthyridine carboxylic acid (**14**, inhibition

**Table 1.** Single concentration screening results of the analogs in the biochemical endonuclease assay, and cell-based antiviral and cytotoxicity assays.

Compound	R <sup>1</sup>	R <sup>2</sup>	 Nuclease inhibition % at 10 μM <sup>[a]</sup>	Cell-based assays [at 10 μM] <sup>[b,c]</sup>	
				Inhibition %	Cell viability %
12	OH	OMe	14 ± 0.5	11 ± 15	98 ± 2.3
13	Cl	OMe	16 ± 2.5	31 ± 2.0	96 ± 1.0
14		OH	19 ± 0.1	16 ± 0.18	97 ± 0.9
15a	Cl		49 ± 4.7	32 ± 7.9	97 ± 2.3
15b	Cl		33 ± 5.3	31 ± 14	95 ± 1.0
15c	Cl		15 ± 2.0	6.8 ± 10	100 ± 5.7
15d	Cl		66 ± 13	51 ± 8.2	96 ± 1.5
15e	Cl		31 ± 8.5	5.9 ± 24	98 ± 0.5
15f	Cl		51 ± 14	7.1 ± 7.9	96 ± 2.1
16a			71 ± 2.4	23 ± 7.1	99 ± 2.6
16b			52 ± 3.6	47 ± 3.9	76 ± 1.7
16c			69 ± 1.6	100 ± 0.1	2.5 ± 0.0
16d			17 ± 8.7	74 ± 19	67 ± 16
16e			8.2 ± 1.9	77 ± 7.0	68 ± 21
17a			25 ± 6.5	21 ± 7.1	98 ± 3.7
17b			53 ± 6.5	20 ± 16	98 ± 4.0

[a] Performed in duplicate and mean is shown. Control compound 6 (10 μM) was included on each plate. A minimum threshold of >80% inhibition was established as a quality control measurement. [b] Control compound GCV (10 μM) was included on each plate. A minimum threshold of >90% inhibition by both controls and no toxicity was established as a quality control measurement. [c] Performed in triplicate and mean is shown.

% = 19) all showed poor inhibition, whereas amide sub-types, including the 5-chloro (**15a–f**), 5-aryl (**16a–e**) and 5-amino analogs (**17a–b**) generally inhibited pUL89-C significantly better (Table 1). However, weak inhibition was observed with a few analogs of the amide subtypes, including 5-chloro amide **15c** (inhibition % = 15), 5-aryl amides **16d** (inhibition % = 17) and **16e** (inhibition % = 8.2), and 5-amino amide **17a** (inhibition % = 25). In parallel to the biochemical screening, all analogs were also screened at 10 μM in an antiviral assay in human foreskin

fibroblasts (HFF) using a GFP-expressing reporter virus, AD-CREGFP. Known HCMV drug GCV (**1**) was used as the control. Similar to the biochemical screening results, non-amide subtypes generally did not inhibit HCMV, whereas most 5-chloro amides, and all 5-aryl and 5-amino amides produced significant antiviral activity (inhibition % ≥ 20) (Table 1), though a few 5-aryl amide analogs (**16c**, **16d**, **16e**) also showed substantial cytotoxicity (viability % ≤ 70) at 10 μM. In general, the screening

assays revealed a good correlation between the biochemical and antiviral potencies.

The biochemical dose-response testing was conducted with all eight compounds showing  $\geq 33\%$  inhibition at  $10\ \mu\text{M}$  in the screening assay. Known pUL89-C inhibitor **6** was used as the control ( $\text{IC}_{50} = 0.5\ \mu\text{M}$ ). Of these eight analogs (Table 2), six ( $\text{IC}_{50} = 1.8\text{--}6.1\ \mu\text{M}$ ) inhibited pUL89-C in single-digit  $\mu\text{M}$  range. Seven of these eight selected compounds were also tested in a dose-response fashion in the cell-based antiviral and cytotoxicity assays. Compound **15f** was excluded due to insignificant

HCMV inhibition at  $10\ \mu\text{M}$ . With the exception of the cytotoxic analog **16c** ( $\text{CC}_{50} = 8.4\ \mu\text{M}$ ), all other six analogs conferred moderate yet consistent antiviral activity in  $\mu\text{M}$  range ( $\text{EC}_{50} = 8.3\text{--}31\ \mu\text{M}$ ) without considerable cytotoxicity ( $\text{CC}_{50} > 50\ \mu\text{M}$ ). Representative dose-response curves for compounds **15a**, **15d**, **16a**, **17b** from the endonuclease assay (A), the antiviral assay (B) and cell viability assay (C) are shown in Figure 3.

### Target protein binding

To assess target binding, pUL89-C protein melting point was measured upon the binding of four selected compounds (**15a**, **15d**, **16a**, **17b**) in the TSA. The observed thermal shift ( $\Delta T_m$ ) indicates the change of  $T_m$  upon compound binding as compared to DMSO control. As shown in the TSA curves (Figure 3, D) all four analogs produced a right shift ( $\Delta T_m > 0$ ), denoting a stabilizing effect by the compounds on pUL89-C. The  $\Delta T_m$  values are shown in Figure 3, E. The smaller shifts observed with these naphthyridine analogs when compared to control compound **6** are consistent with the lower potency in the dose-response endonuclease assay (Table 2).

pUL89-C features a classic DDE motif (D463, E534, and D651) at its active site which chelates two  $\text{Mn}^{2+}$  ions required for the endonuclease activity.<sup>[20]</sup> A reported ligand-bound pUL89-C structure (PDB code: 6EY7<sup>[50]</sup>) allowed us to predict the

Compound	$\text{IC}_{50}$ [ $\mu\text{M}$ ] <sup>[a]</sup>	Cell-based assays <sup>[b]</sup>	
		$\text{EC}_{50}$ [ $\mu\text{M}$ ]	$\text{CC}_{50}$ [ $\mu\text{M}$ ]
<b>15a</b>	$4.3 \pm 1.2$	$8.3 \pm 0.27$	$60 \pm 2.4$
<b>15b</b>	$13 \pm 3.8$	$9.7 \pm 0.14$	$> 50$
<b>15d</b>	$1.8 \pm 0.58$	$21 \pm 0.95$	$> 50$
<b>15f</b>	$5.7 \pm 0.39$	–	–
<b>16a</b>	$2.8 \pm 0.56$	$31 \pm 11$	$> 100$
<b>16b</b>	$24 \pm 5.4$	$24 \pm 9.1$	$> 60$
<b>16c</b>	$6.1 \pm 2.2$	$5.5 \pm 0.42$	$8.4 \pm 0.20$
<b>17b</b>	$2.4 \pm 0.56$	$17 \pm 0.75$	$> 50$
<b>6</b>	$0.52 \pm 0.13$ <sup>[c]</sup>	–	–
<b>1</b> (GCV)	–	$1.6 \pm 0.17$	$> 50$

[a] Performed in duplicate. Compound **6** was used as control. [b] Performed in duplicate. GCV was used as control. [c] Previously reported value:  $\text{IC}_{50} = 1.0\ \mu\text{M}$  [39].

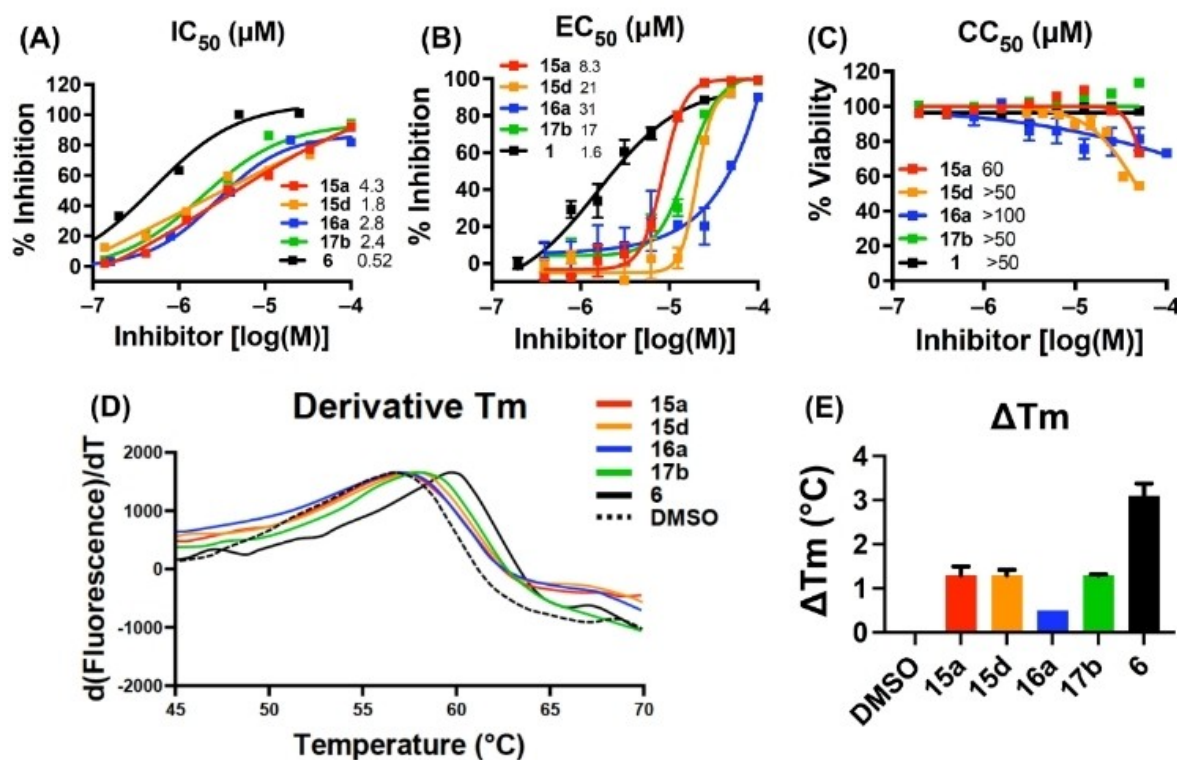


**Figure 3.** Biochemical, antiviral and biophysical characterization of selected analogs **15a**, **15d**, **16a**, **17b**. A) Representative dose-response curves from the biochemical endonuclease assay. Known pUL89-C inhibitor **6** was used as the control; B) dose-response antiviral and C) cell viability testing. GCV (**1**) was used as the control; (D) curves and (E)  $\Delta T_m$  from the TSA.  $\Delta T_m$  was determined independently at least two times with a representative curve shown in (D) and mean  $\Delta T_m$  plus standard deviation shown in (E). Compound **6** was used as the control.

binding nodes of representative analogs via molecular modeling. Figure 4 depicts the preferred binding modes of **15a** and **16a**. Chemically, the two analogs differ mainly at the C5 position where **15a** and **16a** are substituted with a chloro group and a phenyl ring, respectively, resulting in substantially different binding modes (Figure 4). Strikingly, the chelating triad of compound **15a** sits too far away from the two  $\text{Mn}^{2+}$  ions to form the featured metal binding typically expected from such chemotypes. Instead, **15a** binds to the active site via two relatively weak interactions: the  $\pi$ - $\pi$  stacking interaction between F466 and the F-phenyl of the amide moiety (3.3 Å, boxed and red arrow, Figure 4, A); and the  $\pi$ -cation interaction between K583 and the naphthyridine core (4.6 Å, black arrow, Figure 4, A). The weak interactions amount to a poor docking score (XP GScore = -4.44 kcal/mol). By contrast, compound **16a** is predicted to engage with one of the  $\text{Mn}^{2+}$  ions (2.4 Å and 3.1 Å, dotted black line, Figure 4, B), and form an H-bond with T537 (3.3 Å, blue arrow, Figure 4, B). In addition, the  $\pi$ - $\pi$  stacking interaction with F466 and the  $\pi$ -cation interaction with K583 are also predicted (box and black arrow, Figure 4, B). Collectively, these interactions confer a much better docking score (XP GScore = -7.89 kcal/mol). Interestingly, the observed docking scores reflect the same trend as the inhibitory potency from the endonuclease assay ( $\text{IC}_{50}$  = 4.3  $\mu\text{M}$  for **15a** vs  $\text{IC}_{50}$  = 2.8  $\mu\text{M}$  for **16a**, Table 2), though the molecular modeling predicts relatively weak binding at the active site, which corroborates the small shifts observed from the TSA (Figure 3, D & E).

## Conclusion

We have synthesized and tested the 5-chloro (subtype 15), 5-aryl (subtype 16), and 5-amino (subtype 17) subtypes of the 8-hydroxy-1,6-naphthyridine-7-carboxamide chemotype. The initial endonuclease biochemical and antiviral screening assays

identified eight analogs with significant pUL89-C inhibition and antiviral activity, which were further characterized in a dose-response fashion in these assays. Most of the selected analogs inhibited pUL89-C with single-digit  $\mu\text{M}$   $\text{IC}_{50}$  values, and conferred antiviral activity in  $\mu\text{M}$  range. Four of these analogs were also tested in the TSA, where small yet significant right shifts were observed, suggesting that they bind and stabilize pUL89-C. Molecular docking on two selected analogs corroborates pUL89-C binding at the active site. Overall, these biochemical, antiviral, biophysical and *in silico* results support 8-hydroxy-1,6-naphthyridine-7-carboxamide chemotype as a viable inhibitor type of HCMV pUL89-C.

## Experimental Section

### Chemistry

All commercial chemicals were used as supplied unless otherwise indicated. Microwave reactions were carried out in a Biotage Initiator+ w. Robot Eight Microwave System. Compounds were purified via flash chromatography using a Teledyne Combiflash RF-200 with RediSep columns (silica) and indicated mobile phase. All moisture sensitive reactions were performed under an inert atmosphere of ultra-pure argon with oven-dried glassware.  $^1\text{H}$  and  $^{13}\text{C}$  NMR spectra were recorded on a Varian 600 or Bruker 400 MHz spectrometers. Mass data were acquired using an Agilent 6230 TOF LC/MS spectrometer. Procedures for chemical synthesis, analytical characterization data, and original  $^1\text{H}$  and  $^{13}\text{C}$  NMR spectra for all tested compounds are described in Supporting Information.

### In vitro pUL89-C endonuclease assay

pUL89-C was expressed in *E. coli* and purified via a C-terminal histidine tag using nickel affinity chromatography as described.<sup>[20,39]</sup> The 60-bp dsDNA substrate labeled with digoxigenin (DIG) and biotin tags (on 5' and 3' ends, respectively) has been described in detail.<sup>[39,42]</sup> pUL89-C was pre-incubated with compounds in 1% DMSO and reaction buffer (3 mM  $\text{MnCl}_2$ , 30 mM Tris pH 8 and 50 mM NaCl) for 10 min at room temperature. The reaction was

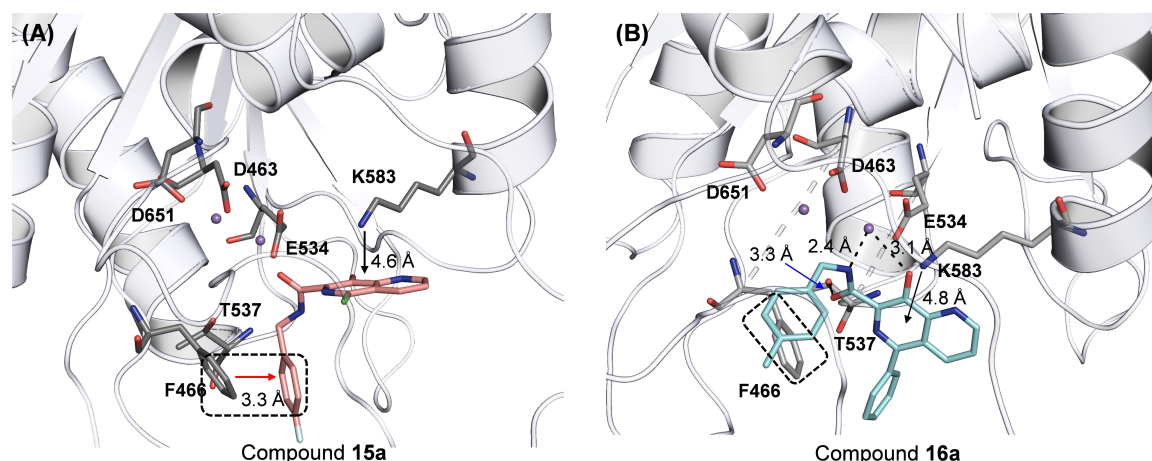


**Figure 4.** Docking poses of representative analogs **15a** and **16a** into HCMV pUL89 active site (PDB code: 6EY7). (A) Predicted binding mode of **15a** (salmon, XP GScore = -4.44 kcal/mol). (B) Predicted binding mode of **16a** (cyan, XP GScore = -7.89 kcal/mol). H-bond and metal chelation are depicted as black dotted lines. Potential  $\pi$ - $\pi$  and  $\pi$ -cation interactions are indicated with arrows. pUL89-C is rendered cartoon in grey. Key residues and ligands are rendered stick, with nitrogen, oxygen, fluorine and chlorine atoms are colored blue, red, cyan, and green, respectively.

initiated by 100 nM dsDNA substrate and incubated for 30 min at 37 °C. The addition of EDTA (final concentration 30 mM) terminated the reaction. The samples were incubated in streptavidin coated plates (Pierce Biotechnology, Rockford, IL) at room temperature with gentle shaking for 30 min and then washed three times with 150  $\mu$ L wash buffer (25 mM Tris, 150 mM NaCl, 0.1% BSA, and 0.05% Tween-20; pH 7.2). Anti-DIG- alkaline phosphatase conjugate antibody (0.15 U/mL) (Roche Applied Sciences, Germany) was added to each well followed by 100  $\mu$ L of p-nitrophenylphosphate (1 mg/mL, Sigma-Aldrich, Saint Louis, MO) as described.<sup>[39,40]</sup> Absorbance of samples were determined at 405 nm using BioTek Neo 2 plate reader. Compound percent inhibition was obtained by comparing signal at a particular dose to the signal obtained by the control sample where no cleavage was observed (EDTA added). The IC<sub>50</sub> was determined using GraphPad Prism 9 software by comparing the percent inhibition for seven serial compound dilutions to the control samples where no cleavage occurs. The IC<sub>50</sub> was defined as the compound concentration resulting in a 50% reduction in substrate signal compared to undigested controls.

### HCMV replication assay

HFF cells (ATCC CRL-2088) were plated in 96-well plates at 1.75  $\times$  10<sup>4</sup> cells/well in DMEM supplemented with 10% fetal bovine serum (FBS), and 1% penicillin streptomycin (P/S). The next day HCMV ADCREGFP virus (obtained from Wade Bresnahan, University of Minnesota) was added at an MOI of 0.01 in DMEM containing 5% FBS and 1% P/S for 2 h. After washing with PBS, test compounds were added to each well (final DMSO concentration 0.5%) and incubated at 37 °C and 5% CO<sub>2</sub> for 7 days. The cells were lysed to measure GFP fluorescence as an indication of the extent of virus replication as described.<sup>[39–40]</sup> GFP relative fluorescence units were determined at excitation/emission 495/515 nm in a BioTek Neo2 plate reader. Samples were performed in triplicate and mean values compared to the mean value for the vehicle control (DMSO alone) wells. Mean percent inhibition for each of the nine serial compound dilutions were compared to DMSO-treated cells and the EC<sub>50</sub> calculated using GraphPad Prism software. EC<sub>50</sub> represents the compound concentration resulting in a 50% reduction in GFP fluorescence (virus replication).

### Cell viability assay

HFF cells were plated into 96-well plates at 1.75  $\times$  10<sup>4</sup> cells/well. Cells were treated the next day with compound in DMSO as described above in the HCMV replication assay except no virus was added. Cellular viability was determined after 7 days using the MTS-based tetrazolium reduction assay CellTiter 96 Aqueous Non-Radioactive cell proliferation assay (Promega) as described.<sup>[40]</sup> Samples were conducted in triplicate and mean values were compared to that for DMSO alone. Mean percent cell viability for each of nine serial compound dilutions was compared to DMSO-treated cells and the CC<sub>50</sub> calculated using GraphPad Prism software. CC<sub>50</sub> was defined as the compound concentration resulting in a 50% reduction in viability.

### pUL89-C thermal shift assay

Test compounds (20  $\mu$ M) were combined with 4  $\mu$ g of purified pUL89-C in reaction buffer (5 mM MnCl<sub>2</sub>, 30 mM Tris pH 8 and 50 mM NaCl) for 25 min at room temperature. Sypro Orange Protein Gel Stain (Sigma Aldrich) was added and the assay conducted as previously described.<sup>[40,42]</sup> All samples were tested in triplicate at a final DMSO concentration of 1%. Protein Thermal Shift Software Version 1.4 from Applied Biosystems was used to determine

melting points and evaluate data. The mean derivative T<sub>m</sub> for the DMSO vehicle control was compared to the mean derivative T<sub>m</sub> of each test compound to calculate the  $\Delta$ T<sub>m</sub>.<sup>[50–51]</sup>

### Molecular modeling

Docking was performed based on the crystal structure of an inhibitor-bound HCMV pUL89-C (PDB code: 6EY7<sup>[50]</sup>). Analogs 15a and 16a were docked using Maestro<sup>[52]</sup> (Schrödinger; LLC: New York, NY, USA) of the Schrödinger small molecule drug discovery suite 2021–3.<sup>[53]</sup> Docking protocols used the standard steps including 1) protein preparation using Protein preparation wizard<sup>[54]</sup> (Schrödinger; LLC: New York, NY, USA), in which only chain A of the tetrameric protein was prepared and minimized using the OPLS3e force field<sup>[55]</sup> to optimize the hydrogen bonding network and converge the heavy atoms to an RMSD of 0.3 Å; 2) receptor grid generation, where the grid was defined in Maestro around the native  $\alpha$ ,  $\gamma$ -diketoacid ligand, covering all the residues within 12 Å; 3) Ligand Preparation, where structures of both analogs were drawn in ChemDraw, saved as sdf, and subjected to LigPrep to generate conformers; and 4) Ligand Docking, where prepared ligands were docked using Glide XP<sup>[56]</sup> (Glide version 8.2). Docked poses were further processed using PyMOL<sup>[57]</sup> (Schrödinger; LLC: New York, NY, USA)

### Acknowledgements

*This research was supported by the National Institute of Allergy and Infectious Diseases, the National Institutes of Health, grant number R01AI136982 (to RJG and ZW). We thank the Minnesota Supercomputing Institute (MSI) at the University of Minnesota for providing molecular modeling resources.*

### Conflict of Interest

The authors declare no conflict of interest.

### Data Availability Statement

The data that support the findings of this study are available in the supplementary material of this article.

**Keywords:** human cytomegalovirus · pUL89-C · endonuclease · inhibitor · 8-hydroxy-1,6-naphthyridine-7-carboxamide

- [1] W. J. Britt, *J. Virol.* **2017**, *91*(15), doi: 10.1128/JVI.02392–02316.
- [2] T. Lazzarotto, D. Blazquez-Gamero, M. L. Delforge, I. Foulon, S. Luck, S. Modrow, M. Leruez-Ville, *Front. Pediatr.* **2020**, *8*, doi:10.3389/fped.2020.00013.
- [3] M. G. Revello, G. Gerna, *J. Clin. Virol.* **2004**, *29*(2), 71–83.
- [4] A. P. Limaye, T. M. Babu, M. Boeckh, *Clin. Microbiol. Rev.* **2020**, *34*(1), doi:10.1128/CMR.00043–00019.
- [5] S. Gianella, S. Letendre, *J. Infect. Dis.* **2016**, *214* Suppl. 2, S67–74.
- [6] R. Perello, A. Vergara, E. Monclus, S. Jimenez, M. Montero, N. Saubi, A. Moreno, Y. Eto, A. Inciarte, J. Mallolas, E. Martinez, M. A. Marcos, *BMC Infect. Dis.* **2019**, *19*(1), doi:10.1186/s12879-12019-14643–12876.
- [7] D. Faulds, R. C. Heel, *Drugs* **1990**, *39*(4), 597–638.
- [8] A. G. Martson, A. E. Edwina, J. G. M. Burgerhof, S. P. Berger, A. de Joode, K. Damman, E. A. M. Verschuuren, H. Blokzijl, M. Bakker, L. F. Span, T. S.

- van der Werf, D. J. Touw, M. G. G. Sturkenboom, M. Knoester, J. W. C. Alffenaar, *J. Antimicrob. Chemother.* **2021**, *76*(9), 2356–2363.
- [9] E. De Clercq, *Clin. Microbiol. Rev.* **2003**, *16*(4), 569–596.
- [10] S. L. Zeichner, *Pediatr. Rev.* **1998**, *19*(12), 399–400.
- [11] T. Goldner, G. Hewlett, N. Ettischer, H. Ruebsamen-Schaeff, H. Zimmermann, P. Lischka, *J. Virol.* **2011**, *85*(20), 10884–10893.
- [12] A. Mullard, *Nat. Rev. Drug Discovery* **2021**, *21*, doi:10.1038/d41573-41021-00208-41572.
- [13] M. N. Prichard, *Rev. Med. Virol.* **2009**, *19*(4), 215–229.
- [14] S. Chou, *Antiviral Res.* **2020**, *176*, 104711.
- [15] S. Chou, K. Song, J. Wu, T. Bo, C. Crumpacker, *J. Infect. Dis.* **2020**, *10.1093/infdis/jiaa1462*.
- [16] S. W. Chou, L. C. Van Wechel, G. I. Marousek, *J. Infect. Dis.* **2007**, *196*(1), 91–94.
- [17] C. M. Douglas, R. Barnard, D. Holder, R. Leavitt, D. Levitan, M. Maguire, D. Nickle, V. Teal, H. Wan, D. van Alewijk, L. J. van Doorn, S. Chou, J. Strizki, *J. Infect. Dis.* **2020**, *221*(7), 1117–1126.
- [18] S. Neuber, K. Wagner, T. Goldner, P. Lischka, L. Steinbrueck, M. Messerle, E. M. Borst, *J. Virol.* **2017**, *91*(12), doi:10.1128/JVI.02384-02316.
- [19] G. Ligat, R. Cazal, S. Hantz, S. Alain, *FEMS Microbiol. Rev.* **2018**, *42*(2), 137–145.
- [20] M. Nadal, P. J. Mas, A. G. Blanco, C. Arnan, M. Sola, D. J. Hart, M. Coll, *Proc. Natl. Acad. Sci. USA* **2010**, *107*(37), 16078–16083.
- [21] K. A. Majorek, S. Dunin-Horkawicz, K. Steczkiewicz, A. Muszewska, M. Nowotny, K. Ginalski, J. M. Bujnicki, *Nucleic Acids Res.* **2014**, *42*(7), 4160–4179.
- [22] W. Yang, *Q. Rev. Biophys.* **2011**, *44*(1), 1–93.
- [23] J. Tang, K. Maddali, M. Metifiot, Y. Y. Sham, R. Vince, Y. Pommier, Z. Wang, *J. Med. Chem.* **2011**, *54*(7), 2282–2292.
- [24] Z. Wang, J. Tang, C. E. Salomon, C. D. Dreis, R. Vince, *Bioorg. Med. Chem.* **2010**, *18*(12), 4202–4211.
- [25] B. Wu, J. Tang, D. J. Wilson, A. D. Huber, M. C. Casey, J. Ji, J. Kankanala, J. Xie, S. G. Sarafianos, Z. Wang, *J. Med. Chem.* **2016**, *59*(13), 6136–6148.
- [26] J. Tang, H. T. Do, A. D. Huber, M. C. Casey, K. A. Kirby, D. J. Wilson, J. Kankanala, M. A. Parniak, S. G. Sarafianos, Z. Wang, *Eur. J. Med. Chem.* **2019**, *166*, 390–399.
- [27] J. Tang, K. A. Kirby, A. D. Huber, M. C. Casey, J. Ji, D. J. Wilson, S. G. Sarafianos, Z. Wang, *Eur. J. Med. Chem.* **2017**, *128*, 168–179.
- [28] J. Tang, F. Liu, E. Nagy, L. Miller, K. A. Kirby, D. J. Wilson, B. Wu, S. G. Sarafianos, M. A. Parniak, Z. Wang, *J. Med. Chem.* **2016**, *59*(6), 2648–2659.
- [29] J. Tang, S. K. V. Vernekar, Y. L. Chen, L. Miller, A. D. Huber, N. Myshakina, S. G. Sarafianos, M. A. Parniak, Z. Wang, *Eur. J. Med. Chem.* **2017**, *133*, 85–96.
- [30] S. K. Vernekar, Z. Liu, E. Nagy, L. Miller, K. A. Kirby, D. J. Wilson, J. Kankanala, S. G. Sarafianos, M. A. Parniak, Z. Wang, *J. Med. Chem.* **2015**, *58*(2), 651–664.
- [31] S. K. V. Vernekar, J. Tang, B. Wu, A. D. Huber, M. C. Casey, N. Myshakina, D. J. Wilson, J. Kankanala, K. A. Kirby, M. A. Parniak, S. G. Sarafianos, Z. Wang, *J. Med. Chem.* **2017**, *60*(12), 5045–5056.
- [32] L. Wang, S. G. Sarafianos, Z. Wang, *Acc. Chem. Res.* **2020**, *53*(1), 218–230.
- [33] L. Wang, J. Tang, A. D. Huber, M. C. Casey, K. A. Kirby, D. J. Wilson, J. Kankanala, M. A. Parniak, S. G. Sarafianos, Z. Wang, *Eur. J. Med. Chem.* **2018**, *156*, 680–691.
- [34] L. Wang, J. Tang, A. D. Huber, M. C. Casey, K. A. Kirby, D. J. Wilson, J. Kankanala, J. Xie, M. A. Parniak, S. G. Sarafianos, Z. Wang, *Eur. J. Med. Chem.* **2018**, *156*, 652–665.
- [35] A. D. Huber, E. Michailidis, J. Tang, M. N. Puray-Chavez, M. Boftsi, J. J. Wolf, K. N. Boschert, M. A. Sheridan, M. D. Leslie, K. A. Kirby, K. Singh, H. Mitsuya, M. A. Parniak, Z. Wang, S. G. Sarafianos, *Antimicrob. Agents Chemother.* **2017**, *61*(6), doi: 10.1128/AAC.00245-00217.
- [36] Y. L. Chen, J. Tang, M. J. Kesler, Y. Y. Sham, R. Vince, R. J. Geraghty, Z. Wang, *Bioorg. Med. Chem.* **2012**, *20*(1), 467–479.
- [37] Y. L. Chen, J. Zacharias, R. Vince, R. J. Geraghty, Z. Wang, *Bioorg. Med. Chem.* **2012**, *20*(15), 4790–4800.
- [38] J. Kankanala, Y. Wang, R. J. Geraghty, Z. Wang, *ChemMedChem* **2018**, *13*(16), 1658–1663.
- [39] Y. Wang, L. Mao, J. Kankanala, Z. Wang, R. J. Geraghty, *J. Virol.* **2017**, *91*(3), doi:10.1128/JVI.02152-02116.
- [40] T. He, T. C. Edwards, J. Xie, H. Aihara, R. J. Geraghty, Z. Wang, *J. Med. Chem.* **2022**, *65*(7), 5830–5849.
- [41] Y. Wang, J. Tang, Z. Wang, R. J. Geraghty, *Antiviral Res.* **2018**, *152*, 10–17.
- [42] L. Wang, T. C. Edwards, R. L. Sahani, J. S. Xie, H. Aihara, R. J. Geraghty, Z. Q. Wang, *Eur. J. Med. Chem.* **2021**, *222*, 10.1016/j.ejmech.2021.113640.
- [43] M. W. Embrey, J. S. Wai, T. W. Funk, C. F. Homnick, D. S. Perlow, S. D. Young, J. P. Vacca, D. J. Hazuda, P. J. Felock, K. A. Stillmock, M. V. Witmer, G. Moyer, W. A. Schleif, L. J. Gabryelski, L. X. Jin, I. W. Chen, J. D. Ellis, B. K. Wong, J. H. Lin, Y. M. Leonard, N. N. Tsou, L. H. Zhuang, *Bioorg. Med. Chem. Lett.* **2005**, *15*(20), 4550–4554.
- [44] J. P. Guare, J. S. Wai, R. P. Gomez, N. J. Anthony, S. M. Jolly, A. R. Cortes, J. P. Vacca, P. J. Felock, K. A. Stillmock, W. A. Schleif, G. Moyer, L. J. Gabryelski, L. X. Jin, I. W. Chen, D. J. Hazuda, S. D. Young, *Bioorg. Med. Chem. Lett.* **2006**, *16*(11), 2900–2904.
- [45] D. J. Hazuda, N. J. Anthony, R. P. Gomez, S. M. Jolly, J. S. Wai, L. H. Zhuang, T. E. Fisher, M. Embrey, J. P. Guare, M. S. Egbertson, J. P. Vacca, J. R. Huff, P. J. Felock, M. V. Witmer, K. A. Stillmock, R. Danovich, J. Grobler, M. D. Miller, A. S. Espeseth, L. X. Jin, I. W. Chen, J. H. Lin, K. Kassahun, J. D. Ellis, B. K. Wong, W. Xu, P. G. Pearson, W. A. Schleif, R. Cortese, E. Emini, V. Summa, M. K. Holloway, S. D. Young, *Proc. Natl. Acad. Sci. USA* **2004**, *101*(31), 11233–11238.
- [46] J. Y. Melamed, M. S. Egbertson, S. Varga, J. P. Vacca, G. Moyer, L. Gabryelski, P. J. Felock, K. A. Stillmock, M. V. Witmer, W. Schleif, D. J. Hazuda, Y. Leonard, L. X. Jin, J. D. Ellis, S. D. Young, *Bioorg. Med. Chem. Lett.* **2008**, *18*(19), 5307–5310.
- [47] M. G. Thomas, M. De Rycker, R. J. Wall, D. Spinks, O. Epemolu, S. Manthri, S. Norval, M. Osuna-Cabello, S. Patterson, J. Riley, F. R. C. Simeons, L. Stojanovski, J. Thomas, S. Thompson, C. Naylor, J. M. Fiandor, P. G. Wyatt, M. Marco, S. Wyllie, K. D. Read, T. J. Miles, I. H. Gilbert, *J. Med. Chem.* **2020**, *63*(17), 9523–9539.
- [48] R. J. Wall, S. Moniz, M. G. Thomas, S. Norval, E. J. Ko, M. Marco, T. J. Miles, I. H. Gilbert, D. Horn, A. H. Fairlamb, S. Wyllie, *Antimicrob. Agents Chemother.* **2018**, *62*(8), e00235–00218.
- [49] L. C. Zhuang, J. S. Wai, M. W. Embrey, T. E. Fisher, M. S. Egbertson, L. S. Payne, J. P. Guare, J. P. Vacca, D. J. Hazuda, P. J. Felock, A. L. Wolfe, K. A. Stillmock, M. V. Witmer, G. Moyer, W. A. Schleif, L. J. Gabryelski, Y. M. Leonard, J. J. Lynch, S. R. Michelson, S. D. Young, *J. Med. Chem.* **2003**, *46*(4), 453–456.
- [50] S. Bongarzone, M. Nadal, Z. Kaczmarek, C. Machon, M. Alvarez, F. Albericio, M. Coll, *ACS Omega* **2018**, *3*(8), 8497–8505.
- [51] A. D. Huber, D. L. Pineda, D. Liu, K. N. Boschert, A. T. Gres, J. J. Wolf, E. M. Coonrod, J. Tang, T. G. Laughlin, Q. Yang, M. N. Puray-Chavez, J. Ji, K. Singh, K. A. Kirby, Z. Wang, S. G. Sarafianos, *ACS Infect. Dis.* **2019**, *5*(5), 750–758.
- [52] Schrödinger *Schrödinger Release 2021–3: Maestro; Schrödinger, LLC: New York, NY, USA, 2021*.
- [53] Schrödinger *Schrödinger Small-Molecule Drug Discovery Suite 2021–3: Schrödinger, LLC: New York, NY, USA, 2021*.
- [54] G. M. Sastry, M. Adzhigirey, T. Day, R. Annabhimoju, W. Sherman, *J. Comput.-Aided Mol. Des.* **2013**, *27*(3), 221–234.
- [55] W. L. Jorgensen, D. S. Maxwell, J. Tirado-Rives, *J. Am. Chem. Soc.* **1996**, *118*(45), 11225–11236.
- [56] R. A. Friesner, R. B. Murphy, M. P. Repasky, L. L. Frye, J. R. Greenwood, T. A. Halgren, P. C. Sanschagrin, D. T. Mainz, *J. Med. Chem.* **2006**, *49*(21), 6177–6196.
- [57] Schrödinger *The PyMOL Molecular Graphics System; Version 2.0: Schrödinger, LLC: New York, NY, USA, 2021*.

Manuscript received: June 20, 2022  
Accepted manuscript online: July 25, 2022  
Version of record online: August 10, 2022